Am. J. Hum. Genet. 69:1186–1197, 2001

The R22X Mutation of the *SDHD* Gene in Hereditary Paraganglioma Abolishes the Enzymatic Activity of Complex II in the Mitochondrial Respiratory Chain and Activates the Hypoxia Pathway

Anne-Paule Gimenez-Roqueplo,[1] Judith Favier,[3] Pierre Rustin,[4] Jean-Jacques Mourad,[5] Pierre-François Plouin,[2] Pierre Corvol,[2,3] Agnès Rötig,[4] and Xavier Jeunemaitre[1,3]

[1]Département de Génétique Moléculaire and [2]Service d'Hypertension Artérielle, Hôpital Européen Georges Pompidou, Assistance Publique/Hôpitaux de Paris, [3]INSERM U36, Collège de France, [4]INSERM U393, Hôpital des Enfants Malades, and [5]Service de Médecine Interne, Hôpital Saint-Michel, Paris

Hereditary paragangliomas are usually benign tumors of the autonomic nervous system that are composed of cells derived from the primitive neural crest. Even though three genes (*SDHD, SDHC,* and *SDHB*), which encode three protein subunits of cytochrome *b* of complex II in the mitochondrial respiratory chain, have been identified, the molecular mechanisms leading to tumorigenesis are unknown. We studied a family in which the father and his eldest son had bilateral neck paragangliomas, whereas the second son had a left carotid-body paraganglioma and an ectopic mediastinal pheochromocytoma. A nonsense mutation (R22X) in the *SDHD* gene was found in these three affected subjects. Loss of heterozygosity was observed for the maternal chromosome 11q21-q25 within the tumor but not in peripheral leukocytes. Assessment of the activity of respiratory-chain enzymes showed a complete and selective loss of complex II enzymatic activity in the inherited pheochromocytoma, that was not detected in six sporadic pheochromocytomas. In situ hybridization and immunohistochemistry experiments showed a high level of expression of markers of the angiogenic pathway. Real-time quantitative reverse transcriptase (RT)–PCR measurements confirmed that vascular endothelial growth factor and endothelial PAS domain protein 1 mRNA levels were significantly higher (three- and sixfold, respectively) than those observed in three sporadic benign pheochromocytomas. Thus, inactivation of the *SDHD* gene in hereditary paraganglioma is associated with a complete loss of mitochondrial complex II activity and with a high expression of angiogenic factors.

Introduction

Paragangliomas are highly vascularized benign tumors derived from neuroectodermal cells. They are preferentially localized in the carotid body. They may be associated with other neural-crest–derived tumors, such as pheochromocytomas. In ~30% of published cases, paragangliomas are inherited. Individuals with familial paragangliomas (MIM 168000, MIM 601650, and MIM 605373) have a more severe presentation (early age at onset and tumors at multiple sites) than do those with sporadic disease. Genetic linkage analyses in several large families have identified loci associated with paraganglioma on 11q23 (*PGL1;* Heutink et al. 1992) and 11q13.1 (*PGL2;* Mariman et al. 1995). Transmission is autosomal dominant with incomplete penetrance when transmitted through fathers, whereas no disease phenotype is observed if transmission is maternal, an observation consistent with maternal genomic imprinting. The third, not maternally imprinted, susceptibility gene was located in 1q21-q23 (*PGL3*) in one German family (Niemann et al. 1999). It has recently been demonstrated that *PGL1* corresponds to the *SDHD* gene, which encodes a mitochondrial respiratory-chain protein of complex II called "cybS" (small subunit of cytochrome *b* in succinate-ubiquinone oxidoreductase) (Baysal et al. 2000). In addition to five nonsense mutations, the authors reported a loss of the maternal allele in tumor DNA, suggesting that *SDHD* is a tumor-suppressor gene that requires two events for inactivation, as hypothesized by Knudson (1986). Then, several germline *SDHD* mutations were reported in families with paraganglioma (Badenhop et al. 2001; Milunsky et al. 2001) and in families with pheochromocytoma (Astuti et al. 2001*a*). The *SDHC* gene encoding the large subunit of cytochrome *b* in succinate-ubiquinone oxidoreductase was reported to correspond to the *PGL3* gene (Niemann and Müller 2000; Niemann et al. 2001). More recently, inactivating *SDHB* gene mutations were also detected in two kindreds (Astuti et al. 2001*b*).

Received September 6, 2001; accepted for publication September 14, 2001; electronically published October 16, 2001.

Address for correspondence and reprints: Dr. Anne-Paule Gimenez-Roqueplo, Département de Génétique Moléculaire, Hôpital Européen Georges Pompidou, 20-40, rue Leblanc, 75015 Paris, France. E-mail: Anne-Paule.GIMENEZ@hop.egp.ap-hop-paris.fr

0002-9297/2001/6906-0004$02.00

Complex II or succinate-ubiquinone reductase (EC 1.3.99.1) is an important enzymatic complex crucial for both the tricarboxylic acid cycle and the aerobic respiratory chains of mitochondria (Saraste 1999). It contains succinate dehydrogenase, with subunits that enable this enzyme to bind directly to the inner mitochondrial membrane. These four nuclear-encoded subunits are composed of two hydrophilic proteins—a flavoprotein (SDHA [70 kD]) and an iron-sulfur protein (SDHB [27 kD]) that form the enzymatic core of the complex—and two hydrophobic integral membrane protein subunits—the large (cybL or SDHC [15 kD]) and small (cybS or SDHD [12 kD]) subunits of cytochrome *b* that anchor the complex. Mitochondria can act as O_2 sensors by increasing the generation of reactive oxygen species, which are required for hypoxia-inducible factor 1 DNA–binding activity and subsequent increases in the synthesis of mRNA that encodes erythropoietin, vascular endothelial growth factor (VEGF), and glycolytic enzymes (Chandel et al. 1998). Because the carotid body contains O_2 chemoreceptors, it has been suggested that chronic hypoxic stimulation could account for the high frequency of sporadic occurrence carotid-body paragangliomas in individuals who live at high altitudes (Pacheco-Ojeda et al. 1988) and for the involvement of the SDHD protein in the pathogenesis of hereditary paraganglioma (Baysal et al. 2000).

In the present study, we investigated the function of a new nonsense mutation in the *SDHD* gene discovered in a family with familial paraganglioma. We used molecular genetics at the germline and somatic levels and in vitro measures of enzymatic activity of the mitochondrial respiratory chain to determine the nature of the genetic defect and to assay its effects on the activity of complex II. We have performed in situ hybridization, immunohistochemistry, and real-time quantitative RT-PCR to evaluate the expression of genes involved in the angiogenic pathway in tumoral tissues.

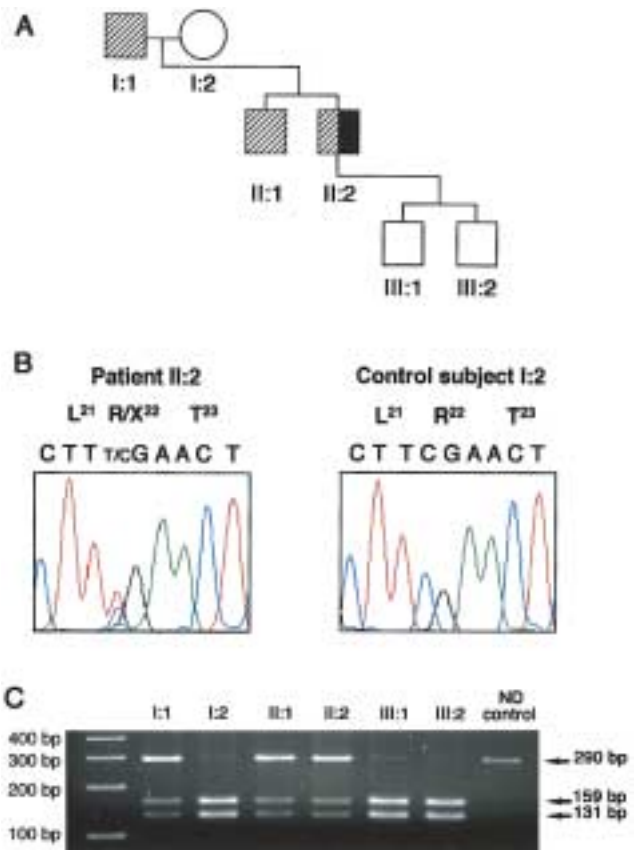

Figure 1 Analysis of mutations in the *SDHD* gene. *A*, Schematic representation of the affected kindred. Paragangliomas are represented by a hatched box and pheochromocytoma by a blackened box. *B*, Sequence analysis of exon 2 of *SDHD* in DNA extracted from the peripheral blood of one affected subject (II:2) and from an unaffected relative (I:2). *C*, Amplification of exon 2 from the blood of all family members and its cleavage with *Bst*BI. The *Bst*BI restriction fragments, obtained after digestion at 65°C for 3 h, were separated by electrophoresis on a 3% agarose gel. The normal maternal allele gave two bands after enzymatic digestion (159 and 131 bp), whereas the paternal mutated allele gave a single undigested band (290 bp). A three-band heterozygous pattern (290, 159, and 131 bp) was observed for patients I:1, II:1, and II:2, whereas the unaffected subjects (I:2, III:1 and III:2) exhibit a two-band homozygous profile. ND = not digested.

Subjects and Methods

Patients

Genetic counseling was offered to a French family that had a history of hereditary paraganglioma. The pedigree of this family is presented in figure 1*A*. Subject I:1 underwent surgery for bilateral carotid-body tumors. His wife (subject I:2) was unaffected by tumors. The first son (subject II:1) had bilateral neck paragangliomas, and the second (subject II:2) had a unilateral glomus tumor with an ectopic mediastinal pheochromocytoma. Clinical examination of the second son's two children (subjects III:1 and III:2) revealed no signs of tumor. Written informed consent was obtained before blood samples were drawn for DNA analysis of each affected and unaffected subject.

Somatic and Constitutive DNA Analysis

DNA was extracted from leukocytes by the classical phenol/chloroform extraction protocol. After removal by surgery, the unfixed ectopic pheochromocytoma from subject II:2 was immediately frozen by immersion in liquid nitrogen. DNA from pheochromocytoma material was extracted using a commercially available kit (RNA/DNA System, Qiagen). The four exons of the *SDHD* gene (GenBank accession number AB 026906) were am-

plified by PCR with primers and a procedure that has been described elsewhere (Baysal et al. 2000). PCR reactions were performed with 3 mM $MgCl_2$ and 0.1 U *Taq*Gold DNA polymerase (Applied Biosystems). The resulting PCR products were directly sequenced using an ABI 3700 fluorescence sequencer (Applied Biosystems). Genotyping of the R22X mutation within the family was performed by forward and reverse sequencing using 2F6610, 5′-CCCCAGTGAAATAGATGCTATC-3′ (forward) and 5′-AGCAGCAGCGATGGAGAGAA-3′ (reverse) primers. The R22X mutation was confirmed by *Bst*BI restriction-enzyme digestion at 65°C for 3 h. The digested amplicons were visualized after electrophoresis in a 3% ethidium bromide–stained agarose gel. The undigested amplicon size was 290 bp; the wild-type allele digested by *Bst*BI yielded two bands (159 and 131 bp).

We investigated whether the *PGL1* locus cosegregated with the disease, using a set of seven fluorescent polymorphic microsatellite 11q markers (D11S987, D11S1314, D11S901, D11S937, D11S4175, D11S898, and D11S908) provided by the ABI Prism Linkage Mapping Set, version 2 (Applied Biosystems). These markers overlap a 10-cM region between 11q13 (*PGL2* locus) and 11q23 (*PGL1* locus). Loss of heterozygosity (LOH) at the *PGL1* locus was investigated with a second set of fluorescent oligonucleotides (D11S1339, D11S1343, D11S5011, D11S5019, D11S1347, D11S908, D11S4111, D11S4104, D11S925, D11S934, D11S4131, D11S4125, and D11S968) (Life Technologies). Amplification conditions were as follows: initial denaturation at 95°C for 10 min, then 35 cycles with 1 min of denaturation at 95°C, 1 min of annealing at 55°C, and 1 min of extension at 72°C, followed by a final extension at 72°C for 30 min. The amplicons were subjected to electrophoresis and were analyzed with an ABI 3700 instrument.

Enzyme Assays

The activities of succinate cytochrome *c* reductase (SCCR) were measured spectrophometrically in tissue homogenates. After we had checked for the absence of germline and somatic mutation of the *SDHD* gene, experiments were performed using six sporadic pheochromocytomas as controls. The activity of the respiratory-chain complexes was measured, as described elsewhere (Rustin et al. 1994). SSCR, reflecting the combined activity of complexes II and III, was measured in medium A, which consists of 10 mM phosphate buffer (pH 7.8), 10 mM succinate, 1 mg/ml bovine serum albumin, 3 μM rotenone (to avoid oxaloacetate production by the malate dehydrogenase, an activity that depends on the recycling of reduced nicotinamide adenine dinucleotide by the respiratory chain), 200 μM adenosine triphosphate, to fully activate the succinate dehydrogenase; and 1 mM potassium cyanide, to avoid cytochrome *c* reoxydation by the cytochrome *c* oxidase. The addition of 40 μM oxidized cytochrome *c* started the reaction. Isolated complex II (EC 1.3.5.1) was measured as the succinate quinone dichlorophenol indophenol (DCPIP) in 1 ml of medium A added with 1 μM DCPIP, and the reaction was started by adding 50 μM decylubiquinone. Under these conditions, electron flow from succinate to quinone requires the functional and structural integrity of the four subunits (A–D) of complex II. The activity of SDH itself (subunit A plus B) was measured by substituting 800 μM phenazine methosulfate (PMS) to decylubiquinone in the presence of 1 mM thenoyltrifluoroacetone, which inhibits electron flow from subunit C to the quinone-acceptor site of complex II. Under these conditions, electron flow from succinate to PMS needs only the functional integrity of subunits A and B of the succinate dehydrogenase (EC 1.3.99.1).

Immunohistochemistry and In Situ Hybridization

Carotid-body paragangliomas (subjects I:1 and II:2) and the ectopic pheochromocytoma (subject II:2) were fixed in formalin and embedded in paraffin. Sections (5–7 μm) were cut and mounted on silane-coated slides. In situ hybridization was performed, as described elsewhere (Sibony et al. 1995), using [^{35}S]-labeled riboprobes produced by in vitro transcription of the following cDNA fragments inserted into pCRII: endothelial PAS domain protein (EPAS) 1 (nucleotides [nt] 512–985), VEGF (nt 1–576), VEGFR-1 (nt 1–1610), VEGFR-2 (nt 57–1387), and Tie2 (nt 52–975). Immunohistochemistry experiments were performed, as described elsewhere (Favier et al. 1999), using an antityrosine hydroxylase antibody (Institut Jacques Boye) at a dilution of 1:1,500, a specific antineurone enolase antibody used at a dilution of 1:1,000 (gift of N. Lamandé) (Legault-Demare et al. 1981) and an anti-HIF1α antibody used at a dilution of 1:1,000 (gift from D. Richard and J. Pouyssegur) (Richard et al. 2000).

Real-Time Quantitative RT-PCR

Total RNA of frozen inherited pheochromocytoma of subject II:2 and of three sporadic pheochromocytomas were extracted with the RNeasy kit (Qiagen), followed by RNAse-free DNAse treatment. The three sporadic pheochromocytomas were used as controls. Direct sequencing of DNA extracted from these tumors showed no *SDHD* mutation, and enzyme assays showed normal SSCR activities. Reverse transcription of 1 μg total RNA was performed in a total volume of 50 μl with 3 mmol/liter $MgCl_2$, 2.5 mmol/liter dNTP mix, 75 mmol/liter KCl, 50 mmol/liter Tris-HCl (pH 8.3), 8.3 mmol/liter DTT, 2.5 μmol/liter random hexamer, 1 U/μl RNAsin,

and 400 U Moloney murine leukemia virus (MMLV) RT. Samples were incubated at 65°C for 15 min, 37°C for 1 h, and 99°C for 3 min. Quantitation of EPAS1 and VEGF cDNAs was performed with a SYBR Green assay, using an ABI Prism 7700 sequence detector (Applied Biosystems). Quantitation of β-actin and 18S ribosomal RNA control cDNAs was also performed with a real-time *Taq*Man PCR assay. For amplification of EPAS1 (GenBank accession number NM 001430), primer sequences are 5′-GCGCTAGACTCCGAGAACAT-3′ (forward) and 5′-TGGCCACTTACTACCTGACCCTT-3′ (reverse). For amplification of VEGF (GenBank accession number NM 003376), primer sequences are 5′-CTACCTCCACCATGCCAAGTG-3′ (forward) and 5′-TGATTCTGCCCTCCTCCTTCT-3′ (reverse). For amplification of β-actin and 18S ribosomal RNA products, primers and probe were purchased directly from Applied Biosystems. Thermocycling conditions were 2 min at 50°C and 10 min of initial denaturation at 95°C, which was followed by 45 cycles of two-step PCR that consisted of 15 s at 95°C and 1 min at 60°C. Duplicate experiments were performed to compare five dilutions (1, 10^{-1}, 10^{-2}, 10^{-3}, and 10^{-4}) of each target cDNA (EPAS1 or VEGF) and five dilutions (1, 10^{-1}, 10^{-2}, 10^{-3}, and 10^{-4}) of each endogenous control (β-actin or 18S ribosomal RNA) for the inherited pheochromocytoma and the three sporadic pheochromocytomas. Relative quantitation of EPAS1 and VEGF gene expression was analyzed as a target-to-control expression ratio, using the standard curve method (Higuchi et al, 1993). The statistical significance of the differential expression between inherited and sporadic pheochromocytomas was assessed by a Mann-Whitney nonparametric test (Staview 5.0., SAS Institute).

Results

Clinical Features of the Family

In this family, tumors were transmitted through the paternal line (fig. 1*A*). The father developed bilateral neck paragangliomas in his sixties. Glomus carotid tumors were diagnosed in his two sons when they were <40 years of age. The clinical history of subject II:2 is remarkable. He underwent surgery in 1998 to remove a left-carotid–body paraganglioma, which was suspected on the basis of self-examination and confirmed by carotid angiogram. Six months after surgery, a blood pressure increase (to 150/100 mm Hg) was observed, together with a fivefold increase in urinary metanephrines (19.4 nmol/24 h). Abdominal computed tomography and whole-body scintigraphy with metaiodobenzyl guanidine detected no tumor. An ectopic pheochromocytoma, 50 mm in diameter, was finally located in the mediastinum behind the heart by octreotide scintigraphy and thoracic computed tomography scan. This corresponded to a 29-g catecholamine-secreting mediastinal paraganglioma, which was surgically removed and had not recurred after 18 mo of follow-up.

Germline and Somatic Analysis of the SDHD *Locus*

Linkage analysis showed a complete father-to-son paternal allele transmission for the seven markers of the chromosome 11q13-q23 region, with no recombination event. Direct sequencing of the four exons of the *SDHD* gene from peripheral DNA of affected subjects showed a C→T nt change in exon 2, creating a premature stop codon in the sequence encoding the signal peptide (R22X) of the mature protein (fig. 1*B*). This heterozygous mutation which was confirmed by *Bst*BI restriction enzymatic digestion (fig. 1*C*), cosegregated with the disease and was not found in 178 normal control chromosomes.

DNA was extracted from the ectopic pheochromocytoma tissue and the *SDHD* gene sequenced. Within the tumor, a loss of the maternal allele was observed for exon 2 of the *SDHD* gene (fig. 2*A*). The deletion of the maternal allele was confirmed by the amplification of exon 2 and its digestion by *Bst*BI. Conversely, biallelic

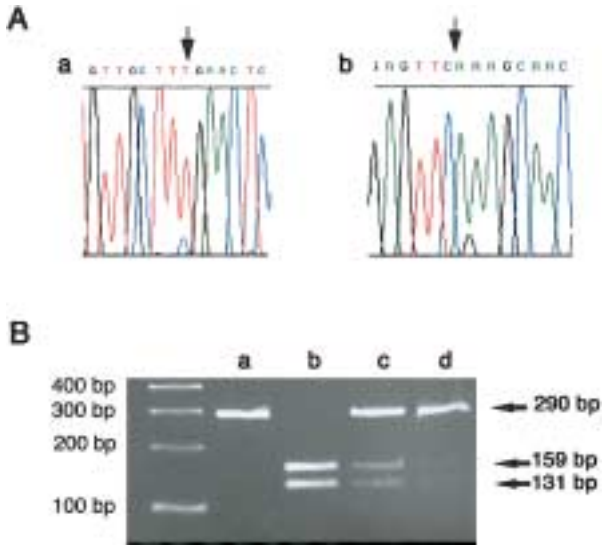

Figure 2 Loss of maternal allele at the *SDHD* gene. *A*, Electrophoretograms corresponding to the forward (*a*) and reverse (*b*) sequences of exon 2 of *SDHD* from the pheochromocytoma of subject II:2. The small peak of C probably results from minor contamination from nontumoral DNA (blood vessel and/or leukocytes). *B*, Amplification of exon 2 and cleavage with *Bst*BI: undigested control (lane a), digested profiles of maternal peripheral DNA (lane b), germline DNA (lane c), and pheochromocytoma DNA (lane d) of subject II:2. The normal maternal allele shows two bands (159 and 131 bp) after digestion and the undigested paternal mutated allele shows one band (290 bp).

expression was observed in leukocytes. In tumor DNA, the maternal allele was lost (fig. 2*B*). To determine the extent of the LOH, 13 regional markers were genotyped in the peripheral and tumor DNA of patient II:2 and were compared with maternal and paternal peripheral DNA (fig. 3). Ten of these markers were informative. An LOH was observed between markers D11S1343 and D11S968, demonstrating a terminal deletion 11q21-q25 of the maternal chromosome

Enzyme-Function Studies

We assessed the activity of respiratory-chain enzymes in the pheochromocytoma developed by subject II:2 and in six sporadic pheochromocytomas that were removed and conserved in the same conditions and for which no mutation of the *SDHD* gene was found. SCCR activity (complex II plus III) was first measured in the control pheochromocytomas (fig. 4*A*). Cytochrome *c* was reduced by succinate, and this reduction was readily inhibited by malonate, a competitive inhibitor of succinate dehydrogenase (fig. 4*C*). After the addition of lauryl maltoside that increases the accessibility of duroquinol and cytochrome *c* to complex III, the addition of duroquinol triggered a rapid reduction of cytochrome *c*. This reduction was essentially inhibited by antimycin, making it possible to estimate complex III activity (QCCR: antimycin-sensitive quinol cytochrome *c* reductase activity or complex III) in the analyzed sample. Similar measurements were made for the pheochromocytoma sample from subject II:2, which showed a complete loss of SCCR activity and an increase in complex III activity (fig. 4*A*). This resulted in the QCCR:SCCR ratio 500 times higher than that for the control pheochromocytomas (fig. 4*A*). Cytochrome oxidase activity was normal in all samples analyzed (data not shown).

We then measured the activity of isolated complex II (SQDR) by using quinone as an electron acceptor, in the presence of cyanide. This activity was abolished in the pheochromocytoma sample from subject II:2 but was detected in control pheochromocytomas (fig. 4*B*). Finally, succinate dehydrogenase activity (SPDR) was measured by following the reduction of phenazine methosulfate (PMSF) by succinate in the presence of thenoyltrifluoroacetone, which blocks electron transfer between the SDH (subunits A plus B) and the respiratory chain. It was also undetectable in the pheochromocytoma sample from subject II:2 (fig. 4*B*). These results demonstrate that this inactivating mutation of the *SDHD* gene in patients with paraganglioma is associated with the complete and selective loss of complex II electron transfer activity and with the loss of the succinate dehydrogenase–mediated step of the Krebs cycle. This complete loss of activity is consistent with somatic loss of the wild-type maternal allele.

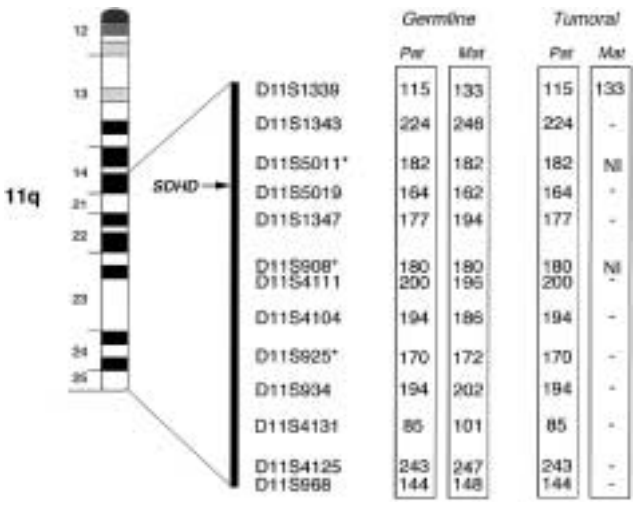

Figure 3 Loss of maternal allele at chromosome 11q21-25. The LOH was typed by microsatellite analysis, using constitutive and tumor DNA from patient II:2. The positions of the markers tested are indicated on an ideogram of chromosome 11. The maternal allele lost is indicated by a line and homozygosity by NI. * = noninformative marker.

Gene Expression Studies

Because the oxidation of mitochondrial cytochromes is known to be a sensor of hypoxia in the glomus carotid body and in cells in general, we thought that complex II mitochondrial chain inactivation might change the expression of genes sensitive to hypoxia and/or encoding angiogenic factors in paragangliomas. The expression of eight genes was studied using in situ hybridization and immunohistochemistry (table 1) in carotid-body paraganglioma (fig. 5) and in pheochromocytoma from subject II:2 (fig. 6). We detected mRNA encoding the transcription factor EPAS1 (HIF2α) (fig. 5*A*) in vascular endothelial cells and also in vascular smooth muscle cells. We observed very large amounts of this transcript within the cell clusters characteristic of paragangliomas ("Zellballen"), in chief cells (type I) of all specimens. Immunostaining with a polyclonal antibody revealed that its homolog, HIF1α, was also detected in these cells (fig. 5*B*). Several putative target genes of these transcription factors were also highly expressed in these tissues. A very strong immunoreactivity was observed for the neurone-specific enolase (NSE), which revealed the Zellballen architecture (fig. 5*D* and 5*I*) of all paragangliomas, as well as in the cells of the pheochromocytoma. This result was expected, because NSE is considered an indicator of neuroendocrine differentiation (Schmechel et al. 1978). The tyrosine hydroxylase (TH) protein was also detected in these cells in all paragangliomas (fig. 5*C*) and was particularly strong in the pheochromocytoma. We observed a high expression of the

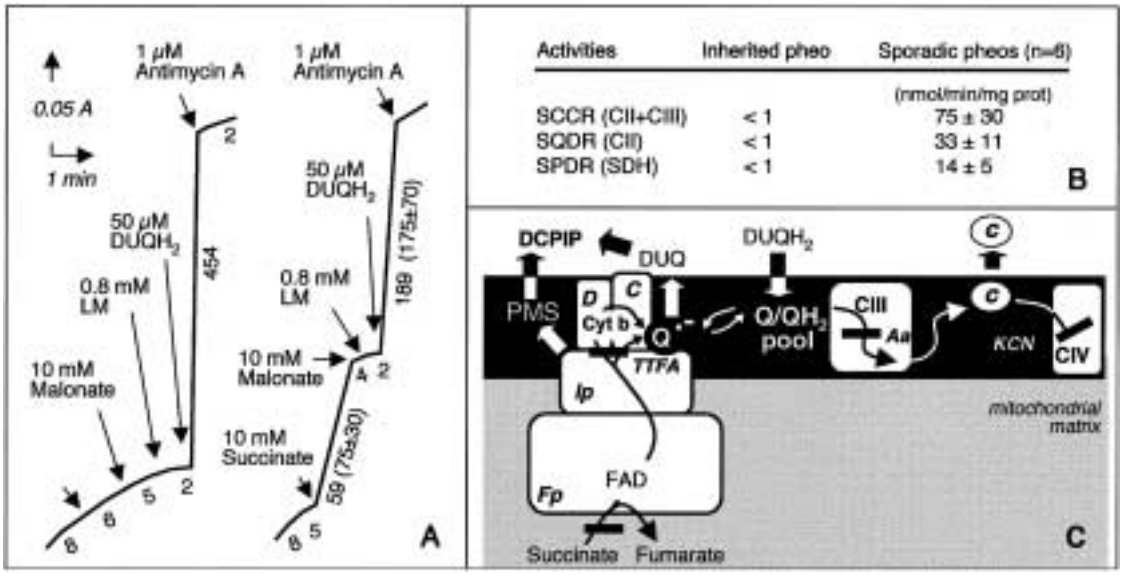

Figure 4 Mitochondrial enzyme function studies. *A*, Spectrophotometric assay of respiratory-chain enzyme activities in tumors with (first trace) and without (second trace) mutations in *SDHD*. The values given on the traces are nmol/min/mg protein. Mean ± 1 SD is indicated in brackets. LM = lauryl maltoside; $DUQH_2$ = decylubiquinol. *B*, Enzyme activities in subject II:2 (inherited pheo) and controls (sporadic pheos). SCCR = malonate-sensitive succinate cytochrome *c* reductase activity (complexes II+III). SQDR = succinate quinone dichlorophenolindophenol reductase (complex II). SPDR = succinate phenazine methosulfate dichlorophenolindophenol reductase (succinate dehydrogenase). *C*, Schematic representation of the principal electron paths through the various subunits of complex II. The acceptor sites for quinones and phenazine methosulfate are indicated as well as the thenoyltrifluoroacetone inhibition site. Aa = antimycin; C = SDHC; CIII = complex III; CIV = complex IV; D = SDHD; DCPIP = dichlorophenolindophenol; DUQ = decylubiquinone; $DUQH_2$ = decylubiquinol; FAD = flavine adenosine; Fp = flavoprotein; Ip = iron protein; KCN = potassium cyanide; PMS = phenazine methosulfate; Q = ubiquinone; $Q^{\bullet-}$ = semiubiquinol; QH_2 = ubiquinol. Q, $Q^{\bullet-}$, and QH_2 are the various forms of the ubiquinone present in the mitochondrial membrane.

VEGF gene in chief cells (fig. 5*E* and 5*J*) and of that encoding its receptor, VEGF-R1 (fig. 5*F* and 5*K*) in endothelial cells from large vessels and capillaries surrounding the Zellballen structures (fig. 5*K*). Higher levels of VEGF-R1 than of VEGF-R2 were detected (fig. 5*G*), particularly in large blood vessels, in which VEGF-R2 was hardly detectable. The Tie2 receptor hybridization signal was at the threshold of detection in vascular endothelial cells (fig. 5*H*).

Interestingly on in situ hybridization experiments, the level of expression of VEGF and of EPAS1 mRNA (fig. 6) was higher in the three carotid-body paragangliomas and in the pheochromocytoma of the family in the present study than those observed in sporadic benign pheochromocytomas. To confirm these observations, we used real-time quantitative RT-PCR to compare the level of EPAS1 and VEGF transcripts in pheochromocytoma from subject II:2 and three sporadic pheochromocytoma controls who had no *SDHD* mutation and a normal SDH activity. As indicated in figure 7, there was, on average, a sixfold increase in the level of EPAS1 mRNAs and a threefold increase of VEGF mRNAs whatever the endogenous RNA control used. The statistical significance of these results was demonstrated using a Mann-Whitney statistical test: $z = -2.910$, $P = .0036$ for all combinations (EPAS1 vs. β-actin, EPAS1 vs. 18S, VEGF vs. β-actin, and VEGF vs. 18S).

Discussion

The mitochondrial respiratory chain is a protein complex of potential interest in oncogenesis, especially after the discovery that the *SDHD* gene corresponds to the *PGL1* locus (Baysal et al. 2000). The present study not only confirms the role of the *SDHD* gene in hereditary paraganglioma but also shows that the induced defect in the complex II mitochondrial chain is associated with the overproduction of angiogenic factors, which may in turn stimulate angiogenesis and therefore tumor growth.

Three different loci have been implicated in familial paraganglioma. The inheritance pattern of these genes is usually consistent with autosomal dominant transmission with maternal genomic imprinting (Van der Mey et al. 1989). Indeed, the children of affected fathers developed tumors, whereas the children of affected mothers remained tumor free. Several authors have suggested that an epigenetic modification, such as the methylation of CpG islets on parental chromosomes might confer a reversible difference on the maternal and paternal chromosomes during gametogenesis (Van der

Table 1

Semiquantitative Assessment of In Situ Hybridization and Immunohistochemistry Observations

	In Situ Hybridization					Immunohistochemistry		
Subject and Tumor	EPAS1	VEGF	VEGF-R1	VEGF-R2	Tie2	HIF1α	NSE	TH
I:1								
Right paraganglioma	+++	+++	+++	+++	+	++	++	++
Left paraganglioma	++	++++	+++	+++	+	+	+++	+
II:2								
Paraganglioma	+++	+++	++++	+++	+	++	+++	++
Pheochromocytoma	+++	+++	++++	+++	+	++	++	++++

Note.—Relative intensities of the markers studied are represented for the three carotid-body paragangliomas (in subjects I:1 and II:2) and the pheochromocytoma (in subject II:2). Labeling intensity was evaluated twice in a blinded manner and was graded using a 5-scale system: − = no signal; + = weak; ++ = moderate; +++ = strong; ++++ = very strong.

Mey et al. 1989; Milunsky et al. 1997). This modification could affect a tissue-specific promoter (Pfeifer, 2000). This hypothesis is consistent with biallelic expression of the *SDHD* gene in tumor tissue. Nonetheless, our data provide no evidence for maternal imprinting but instead suggest an LOH in tumor tissue, consistent with Knudson's classical two-hit hypothesis for the induction of tumor formation (Knudson 1986). Conversely, we were able to detect biallelic expression of the *SDHD* gene and normal complex II activity in adrenal tissue in two other sporadic pheochromocytomas (data not shown).

Tumor prognosis probably differs with the function and number of deleted genes. A high frequency of 11q loss in familial paragangliomas, similar to the loss in the family described here, was recently reported elsewhere (Dannenberg et al. 2001). Several of the genes surrounding *SDHD* on human chromosome 11q21-q25, may be involved in tumorigenesis (Koreth et al. 1999; Baysal et al. 2001). One of them is the *PPP2R1B* gene which is separated from *SDHD* by only 250 kb on the physical map. This putative tumor-suppressor gene, which encodes the β isoform of the A subunit of serine/threonine protein phosphatase 2A, has been implicated in human lung and colon cancer (Wang et al. 1998). Therefore, it will be important to study the phenotype-genotype relationships in several families with paraganglioma to determine whether the size and location of the somatic deletions are associated with a higher risk of malignancy in paraganglioma and sporadic pheochromocytoma induced by *SDHD* mutations (Gimm et al. 2000).

It has been suggested that mitochondria are the primary site of oxygen sensing in the carotid body (Prabhakar. 2000). Mitochondria produce cellular energy by a process of oxidative phosphorylation involving five respiratory-enzyme complexes. Complex II transfers electrons from succinate to the ubiquinone pool. Isolated complex II deficiency has been reported in Leigh syndrome. The causative mutation was identified in the *SDHA* gene encoding the flavoprotein of complex II, and the enzymatic defect was partial (Bourgeron et al. 1995). No associated tumor was detected in this family (A.R. and P.R., unpublished data). In *Caenorhabditis elegans*, a mutant of *mev-1* gene that is homologous to the human *SDHC* gene has been found to be hypersensitive to high oxygen concentrations. In *mev-1* mutant animals, the ability of complex II to catalyze electron transport from succinate to ubiquinone is compromised, indirectly causing an increase in superoxide levels and premature aging (Ishii et al. 1998). Surprisingly enough, succinate dehydrogenase (subunits A and B), assumed to be not inserted in the mitochondrial membrane, was found still active despite the loss of the anchoring subunits in *mev-1* mutant animals. These observations contrast with numerous cases where the absence (or even the mutation) of one subunit in a given respiratory-chain complex results in the destabilization of the complex and the subsequent proteolysis of the noninserted subunits (Birch-Machin et al. 1996; Bruno et al. 1999; Clark et al. 1999). Our studies of human pheochromocytomas did not confirm the observation made in the nematode. The defect in one of the anchoring subunits is predicted to result in the noninsertion of the SDH and presumably to its proteolysis. Accordingly, mutation in the *SDHD* gene of subject II:2 resulted in the complete loss of both the catalytic activity of succinate dehydrogenase (subunits A plus B) and electron flow from succinate to the ubiquinone pool, which requires all complex II subunits. The complete abolition of complex II activity resulting from a heterozygous constitutive mutation of the *SDHD* gene associated with a somatic maternal LOH, as described in the pheochromocytoma of this family, has not been reported before.

This dramatic disturbance of the mitochondria respiratory chain accounts for the hypoxic status of the cells and probably explains the high level of expression of genes encoding hypoxia induced factors. Jyung et al. (2000) reported the detection of positive immunohistochemical staining for VEGF in 65% of sporadic glo-

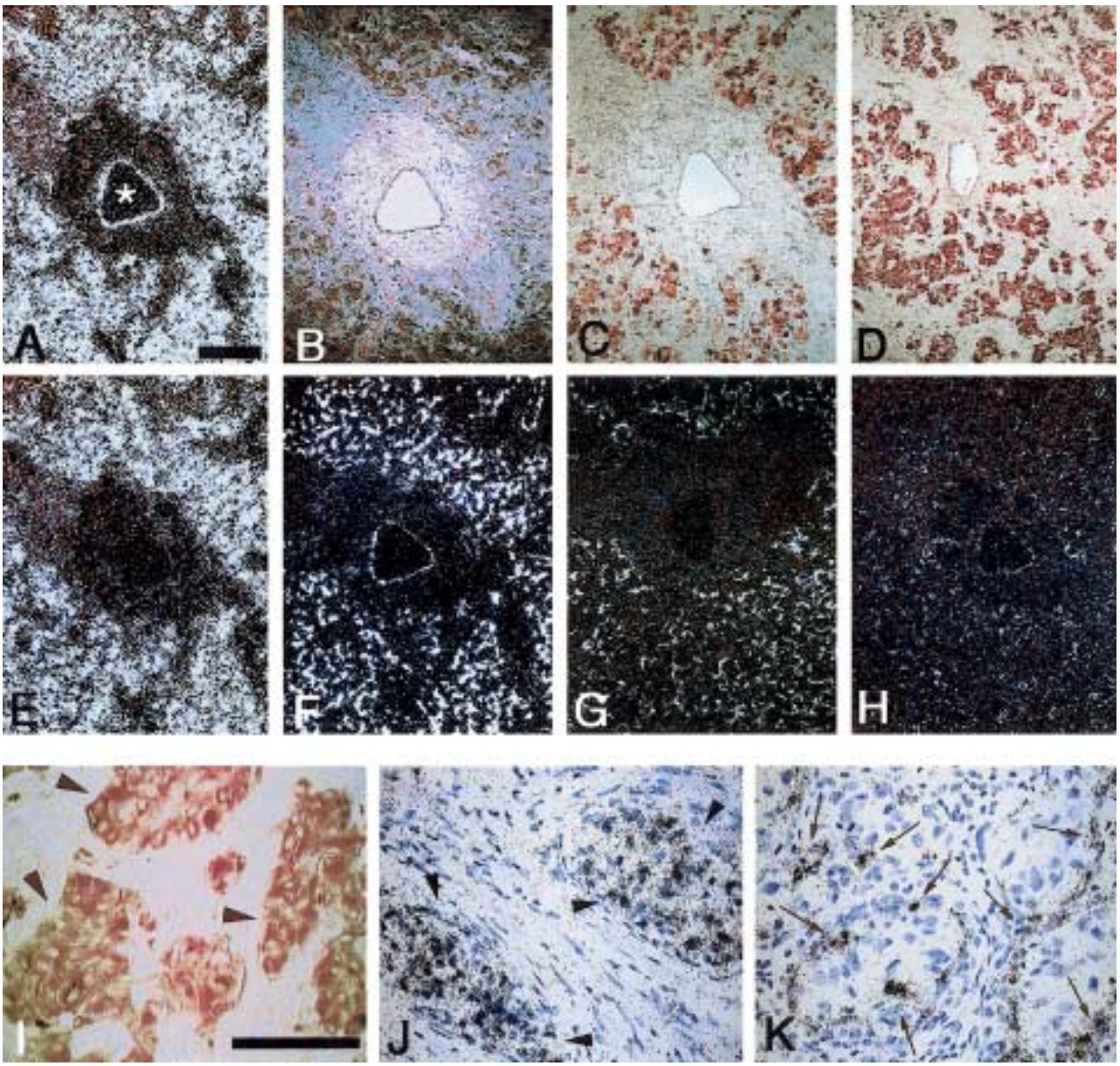

Figure 5 Gene-expression patterns in right carotid-body paraganglioma of patient I:1, as shown by in situ hybridization or immunostaining. EPAS1 mRNA is observed in both endothelial cells and tumor cells (*A*). The protein of the homolog transcription factor HIF1α is also present (*B*). Tyrosine hydroxylase (*C*), NSE (*D* and *I*) and VEGF (*E* and *J*) are present at a very high level in tumor cells within the Zellballen clusters, whereas VEGF receptors R1 (*F* and *K*) and R2 (*G*) transcripts are restricted to endothelial cells. Note the absence of VEGF-R2 in the wall of the central large vessel (*) and the almost undetectable signal with the Tie2 probe (*H*). High magnifications clearly reveal the expression of NSE (*I*) and VEGF (*J*) within the Zellballen structures (*arrowheads*), surrounded by a VEGF-R1 positive capillary network (*K*, *arrows*). The in situ hybridization signals are visualized either under dark (*A* and *E–H;* signal visible as white dots) or bright field illumination (*J* and *K*;labeling detected by black dots). Immunostaining (*B*, *D*, and *I*) is revealed by a brown coloration. Scale bars = 200 μm (*A–H*); scale bars = 100 μm (*I–K*).

mus paraganglioma studied. We have confirmed and extended these results in inherited paragangliomas by describing the expression pattern of several angiogenic markers that may be involved in tissue adaptation to hypoxia. We have shown, in these tumors, the strong expression of hypoxia-inducible transcription factors (EPAS1/HIF2α and HIF1α) and genes encoding some of the targets of these factors. The hybridization signal for EPAS1 and for VEGF and its receptor VEGF-R1 was particularly strong in these tumors. We made two important observations that suggest a direct link between the high expression of genes encoding angiogenic

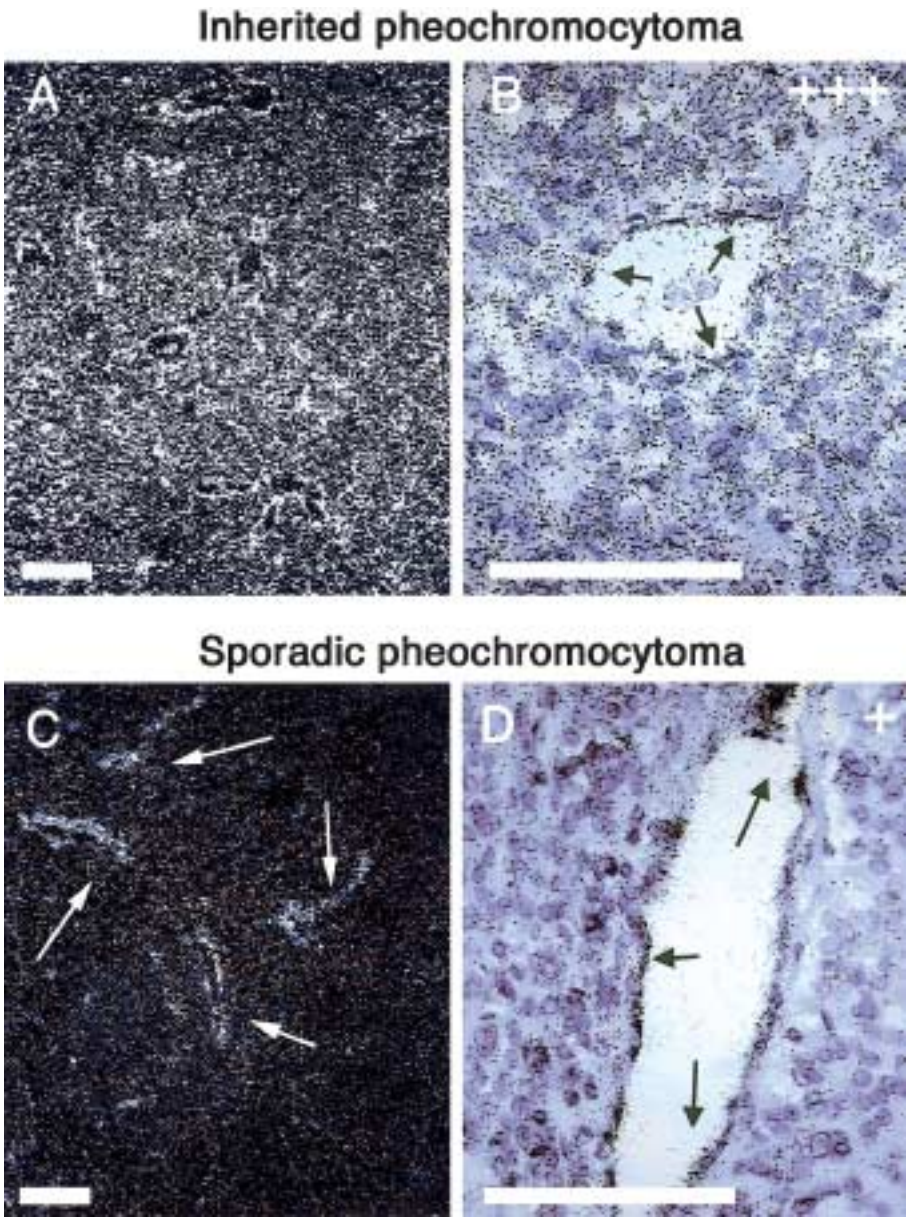

Figure 6 EPAS1 mRNA expression; comparison between patient II:2 pheochromocytoma and a sporadic benign pheochromocytoma. The expression of EPAS1 within tumor cells is higher in the inherited pheochromocytoma (*A* and *B*) than in a sporadic pheochromocytoma (*C* and *D*). In contrast, the intensity of EPAS1 signal does not vary between the two samples in endothelial cells (*black arrows*). The in situ hybridization signals are observed under dark-field illumination for low magnifications (*A* and *C* [white dots]) and under bright field illumination for enlargements (*B, D* [black dots]). White arrows = blood vessels; +++ = very strong signal; + = weak signal. Scale bars = 100 μm.

factors and the loss of SDHD function. First, VEGF-R1 mRNA, which encodes the VEGF receptor induced in hypoxic conditions (Gerber et al. 1997), was found to be more abundant than VEGF-R2 mRNA. Second, the level of EPAS1 and VEGF labeling observed in the three paraganglioma tumors and in the pheochromocytoma of this family was stronger than that observed in sporadic benign pheochromocytomas. These observations were confirmed by quantitative RT-PCR experiments which revealed a higher expression of both genes in patient II:2 pheochromocytoma than in three sporadic pheochromocytomas, with no *SDHD* mutation and a normal SDH activity. The mutation in the *SDHD* gene is therefore probably involved in induction of the hypoxia/angiogenesis response and possibly in tumor development. However, it is unclear whether the activation of hypoxia pathways is or is not sufficient to induce tumorigenesis by itself. It remains possible that other

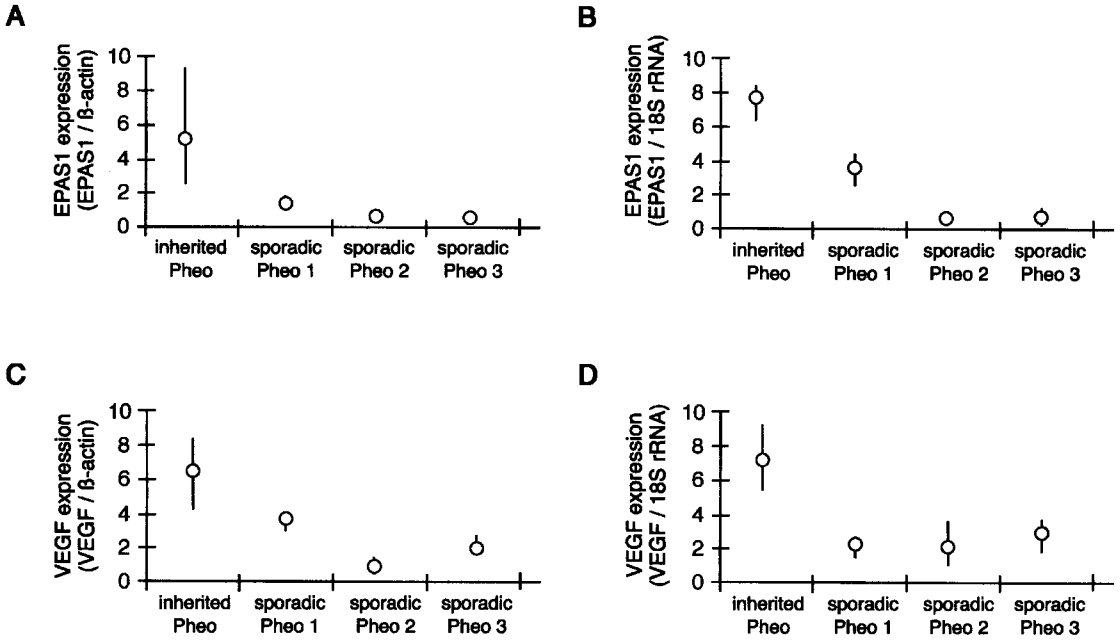

Figure 7 Real-time quantitative RT-PCR experiments. The level of EPAS1 and VEGF transcripts were compared between the *SDHD* mutated pheochromocytoma (inherited Pheo) with three sporadic pheochromocytomas (sporadic Pheo 1, 2, and 3). Comparison of quantitative DNA data obtained with EPAS1 as target and β-actin (*A*) or 18S ribosomal RNA (*B*) as endogenous control and of data obtained with VEGF as target and β-actin (*C*) or 18S ribosomal RNA (*D*) as endogenous controls. The circle represents the mean of 10 calculated measurements (ratio of target gene on reference gene for each of five log of concentration in duplicate). The superior bar shows the maximal value, and the inferior bar shows the minimal value.

functions, downstream from *SDHD*, are impaired in these cells and/or that genes other than *SDHD* are also affected (e.g., *PPP2R1B*).

Recent identification of mutations in the *SDHD*, *SDHC* and *SDHB* genes as responsible for familial paraganglioma has added to the molecular tools available for genetic counseling, which was previously based on indirect testing using microsatellite markers from chromosome 11q13 and 11q23 (Oosterwijk et al. 1996; Bikhazi et al. 1999; Petropoulos et al. 2000). Genetic diagnosis can now be made by direct sequencing to search for a causative mutation in these three genes, even in families with few affected members. The discovery of a genomic mutation in a patient with paraganglioma is important for the genetic counseling of his or her family, including predictive DNA testing mutations in all relatives and screening for paraganglioma at a presymptomatic stage. Indeed, the early detection of paraganglioma reduces the incidence of morbidity and mortality (Petropoulos et al. 2000).

In conclusion, this study shows that somatic loss of maternal allele of the *PGL1* locus, together with inherited paternal mutation of the *SDHD* gene, is responsible for a complete loss of activity of the complex II of the mitochondrial respiratory chain and is associated with a stimulation of angiogenic factors that might in turn facilitate or trigger tumorigenesis in paraganglial tissues.

Acknowledgments

We thank Dr. Jean-Marie Gasc, for helpful discussions of the manuscript, Dr. N. Lamandé, Dr. D. Richards, and Dr. J. Pouyssegur, for antibodies. The English text was edited by Dr. J. Sappa. This study was supported by INSERM and by PHRC grant AOM 95201, for the COMETE Network.

Electronic-Database Information

Accession numbers and URLs for data in this article are as follows:

GenBank, http://www.ncbi.nlm.nih.gov/Genbank (for the sequence of *SDHD*)

Online Mendelian Inheritance in Man (OMIM), http://www.ncbi.nlm.nih.gov/Omim/ (for reviews of familial paragangliomas)

References

Astuti D, Douglas F, Lennard TWJ, Aligianis IA, Woodward ER, Evans GR, Eng C, Latif F, Maher ER (2001*a*) Germline SDHD mutation in familial phaeochromocytoma. Lancet 357:1181–1182

Astuti D, Latif F, Dallol A, Dahia PL, Douglas F, George E, Skoldberg Husebye ES, Eng C, Maher ER (2001*b*) Gene mutations in the succinate dehydrogenase subunit SDHB cause susceptibilty to familial pheochromocytoma and to familial paraganglioma. Am J Hum Genet 69:49–54

Badenhop RF, Cherian S, Lord RS, Baysal BE, Taschner PE, Schofield PR (2001) Novel mutations in the SDHD gene in pedigrees with familial carotid body paraganglioma and sensorineural hearing loss. Genes Chromosomes Cancer 31: 255–263

Baysal BE, Ferrell RE, Willett-Brozick JE, Lawrence EC, Myssiorek D, Bosch A, Van Der Mey A, Taschner PEM, Rubinstein WS, Myers EN, Richard CW 3d, Cornelisse CJ, Devilee P, Devlin B (2000) Mutations in SDHD, a mitochondrial complex II gene, in hereditary paraganglioma. Science 287: 848–851

Baysal BE, Willett-Brozick JE, Tascner PEM, Dauwerse JG, Devilee P, Devlin B (2001) A high-resolution integrated map spanning the SDHD gene at 11q23: a 1.1-Mb BAC contig, a partial transcript map and 15 new repeat polymorphisms in a tumor suppressor region. Eur J Hum Genet 9:121–129

Bikhazi PH, Roeder E, Attaie A, Lalwani AK (1999) Familial paragangliomas: the emerging impact of molecular genetics on evaluation and management. Am J Otol 20:639–643

Birch-Machin M, Marsac C, Ponsot G, Parfait B, Taylor RW, Rustin P, Munnich A (1996). Biochemical investigations and immunoblot analysis of two unrelated patients with an isolated deficiency in complex II of the respiratory chain. Biochem Biophys Res Commun 220:57–62

Bourgeron T, Rustin P, Chretien D, Birch-Machin M, Bourgeois M, Viegas-Pequignot E, Munnich A, Rotig A (1995) Mutation of a nuclear succinate dehydrogenase gene results in mitochondrial respiratory chain deficiency. Nat Genet 11: 144–149

Bruno C, Martinuzzi A, Tang Y, Andreu AL, Palloti F, Bonilla E, Shanske S, Fu J, Sue CM, Angelini C, DiMauro S, Manfredi G (1999) A stop-codon mutation in the human mtDNA cytochrome *c* oxidase I gene disrupts the functional structure of complex IV. Am J Hum Genet 65:611–620

Chandel NS, Maltepe E, Goldwasser E, Mathieu CE, Simon MC, Schumacker PT (1998) Mitochondrial reactive oxygen species trigger hypoxia-induced transcription. Proc Natl Acad Sci USA 95:11715–11720

Clark KM, Taylor RW, Johnson MA, Chinnery PF, Chrzanowska-Lightowlers ZM, Andrews RM, Nelson IP, Wood NW, Lamont PJ, Hanna MG, Lightowlers RN, Turnbull DM (1999) An mtDNA mutation in the initial codon of the cytochrome *c* oxidase subunit II gene results in lower levels of the protein and a mitochondrial encephalomyopathy. Am J Hum Genet 64:1330–1339

Dannenberg H, Krijger RR, Zhao J, Speel EJM, Saremaslani P, Dinjens WNM, Mooi WJ, Roth J, Heitz PU, Komminoth P (2001) Differential loss of chromosome 11q in familial and sporadic parasympathetic paragangliomas detected by comparative genomic hybridization. Am J Pathol 158: 1937–1942

Favier J, Kempf H, Corvol P, Gasc JM (1999) Cloning and expression pattern of EPAS1 in the chicken embryo: colocalization with tyrosine hydroxylase. FEBS Lett 462:19–24

Gerber HP, Condorelli F, Park J, Ferrara N (1997) Differential transcriptional regulation of the two vascular endothelial growth factor receptor genes. Flt-1, but not Flk-1/KDR, is up regulated by hypoxia. J Biol Chem 272:23659–23667

Gimm O, Armanios M, Dziema H, Neumann HP, Eng C (2000) Somatic and occult germ line mutations in SDHD, a mitochondrial complex II gene, in nonfamilial pheochromocytoma. Cancer Res 60:6822–6825

Heutink P, Van der Mey AG, Sandkuijl LA, Van Gils AP, Bardoel A, Breedveld GJ, Van Vliet M, Van Ommen GJ, Cornelisse CJ, Oostra BA, Weber JL, Devilee P (1992) A gene subject to genomic imprinting and responsible for hereditary paragangliomas maps to chromosome 11q23-qter. Hum Mol Genet 1:7–10

Higuchi R, Fockler C, Dollinger G, Watson R (1993) Kinetic PCR analysis: real-time monitoring of DNA amplification reactions. Biotechnology 11:1026–1030

Ishii N, Fujii M, Hartman PS, Tsuda M, Yasuda K, Senoo-Matsuda N, Yanase S, Ayusawa D, Suzuki K (1998) A mutation in succinate dehydrogenase cytochrome *b* causes oxidative stress and ageing in nematodes. Nature 394:694–697

Jyung RW, LeClair EE, Bernat RA, Kang TS, Ung F, McKenna MJ, Tuan RS (2000) Expression of angiogenic growth factors in paragangliomas. Laryngoscope 110:161–167

Knudson AG (1986) Genetics of human cancer. Annu Rev Genet 20:231–251

Koreth J, Bakkenist CJ, McGee JO (1999) Chromosomes, 11q and cancer: a review. J Pathol 187:28–38

Legault-Demare L, Lamande N, Zeitoun Y, Gros F, Scarna H, Keller A, Lando D, Cousin MA (1981) Transition between isozymic forms of enolase during in vitro differentiation of neuroblastoma cells-II. Neurochem Int 3:301–310

Mariman ECM, Van Beersum SEC, Cremers CWRJ, Struycken PM, Ropers HH (1995) Fine mapping of a putatively imprinted gene for familial non-chromaffin paragangliomas to chromosome 11q13.1: evidence for genetic heterogeneity. Hum Genet 95:56–62

Milunsky JM, DeStefano A, Huang XL, Baldwin C, Michels V, Jako G, Milunsky A (1997) Familial paragangliomas: linkage to chromosome 11q23 and clinical implications. Am J Med Genet 72:66–70

Milunsky JM, Maher TA, Michels VV, Milunsky A (2001) Novel mutations and the emergence of a common mutation in the SDHD gene causing familial paraganglioma. Am J Med Genet 100:311–314

Niemann S, Steinberger D, Müller U (1999) PGL3, a third, not maternally imprinted locus in autosomal dominant paraganglioma. Neurogenetics 2:167–170

Niemann S, Müller U (2000) Mutations in SDHC cause autosomal dominant paraganglioma, type 3. Nat Genet 26: 268–270

Niemann S, Becker-Follmann J, Nürnberg G, Rüschendorf F, Sieweke N, Hügens-Penzel M, Traupe H, Wienker TF, Reis A, Müller U (2001) Assignment of PGL3 to chromosome 1(q21-q23) in a family with autosomal dominant non-chromaffin paraganglioma. Am J Med Genet 98:32–36

Oosterwijk J, Jansen J, Van Schothorst E, Oosterhof A, Devilee P, Bakker E, Zoeteweij M, Van der Mey A (1996) First experiences with genetic counselling based on predictive

DNA diagnosis in hereditary glomus tumours (paragangliomas). J Med Genet 33:379–383

Pacheco-Ojeda L, Durango L, Rodriguez C, Vivar N (1988) Carotid body at high altitudes. World J Surg 12:856–860

Petropoulos AE, Luetje CM, Camarata PJ, Whittaker CK, Lee G, Baysal BE (2000) Genetic analysis in the diagnosis of familial paragangliomas. Laryngoscope 110:1225–1229

Pfeifer K (2000) Mechanisms of genomic imprinting. Am J Hum Genet 67:777–787

Prabhakar NR (2000) Oxygen sensing by the carotid body chemoreceptors. J Appl Physiol 88:2287–2295

Richard DE, Berra E, Pouyssegur J (2000) Nonhypoxic pathway mediates the induction of hypoxia-inducible factor 1 α in vascular smooth muscle cells. J Biol Chem 275: 26765–26771

Rustin P, Chretien D, Bourgeron T, Gerard B, Rotig A, Saudubray JM, Munnich A (1994) Biochemical and molecular investigations in respiratory chain deficiencies. Clin Chim Acta 228:35–51

Saraste M (1999) Oxidative phosphorylation at the fin de siecle. Science 283:1488–1493

Schmechel D, Marangos PJ, Brightman M (1978) Neurone-specific enolase is a molecular marker for peripheral and central neuroendocrine cells. Nature 276:834–836

Sibony M, Commo F, Callard P, Gasc JM (1995) Enhancement of mRNA in situ hybridization signal by microwave heating. Lab Invest 73:586–591

Van Der Mey AGL, Maaswinkel-Moy PD, Cornelisse CJ, Schmidt PH, Van de Kamp JJP (1989) Genomic imprinting in hereditary glomus tumours: evidence for new genetic theory. Lancet 2:1291–1294

Wang SS, Esplin ED, Li JL, Huang L, Gazdar A, Minna J, Evans GA (1998) Alterations of the PPP2R1B gene in human lung and colon cancer. Science 282:284–287